Solar energy in production of L-glutamate through visible light active photocatalyst—redox enzyme coupled bioreactor†

Chan Beum Park,[a] Sahng Ha Lee,[a] Esakkiappan Subramanian,[b] Bharat. B. Kale,[c] Sang Mi Lee[d] and Jin-Ook Baeg*[d]

Received (in Cambridge, UK) 15th May 2008, Accepted 22nd August 2008
First published as an Advance Article on the web 20th September 2008
DOI: 10.1039/b808256a

A new potentially promising visible-light driven photobioreactor synthesizes fine chemical *via* photobiocatalysis by generating NADH in a non-enzymatic light-driven process and coupling it to the enzymatic dark reaction catalysis.

Nature utilizes solar energy for the synthesis of various organic chemicals, which remains as a target model for the development of artificial photosynthesis systems.[1] Natural photosynthesis through the Z scheme of two photosystems,[2] testifies an elegant example of how a fine nexus between photocatalysis and biocatalysis could be designed in a heterogeneous phase. Devising an artificial analogue in the heterogeneous phase has been a long-standing challenge in chemistry.[3] The present work attempts the construction of such a photobioreactor device using a semiconductor photocatalyst through the integral coupling of photocatalysis and biocatalysis cycles. It unites these two catalytic functionalities in a novel photobiocatalytic system for the ultimate goal of utilizing solar energy in the visible region for photobiosynthesis of fine chemicals. Since energetically 46% of total solar light available on Earth is in the visible range and only 4% in the UV range,[4] it is imperative that the photocatalysis must be visible light functional for a real and meaningful solar energy conversion.

In biocatalytic systems, many enzymes depend on nicotinamide co-factors (NAD and NADP) for their functions. The high cost of these co-factors, however, is prohibitive of industrialization of many promising enzymatic processes.[5–7] Therefore, an efficient method of their *in situ* regeneration is the only means for making the processes economically and industrially feasible.[6–8] In the regeneration of co-factors, so far, a number of strategies involving enzymes have been investigated,[6–9] but are still associated with their own drawbacks.[6,10,11] Through the use of photochemical energy, an alternative strategy is envisioned for the regeneration of co-factors, which also provides the opportunity of harnessing clean and abundant solar energy.[8]

Photochemical co-factor regenerations, with a few studies to date either in homogeneous (soluble pigment sensitizer[12]) or heterogeneous (TiO_2/CdS photocatalyst[8,13]) phase have used enzyme mediators and, therefore, suffer from drawbacks such as low specific activity and yield, substrate inhibition and high cost.[6] In addition, they also have other drawbacks of photocatalyst instability,[8] difficulty in isolation/separation of co-factor from the homogeneous medium, poisonous electron relay (methyl viologen) *etc*.[6,8] All these associated shortcomings make the previously studied photocatalytic systems unsatisfactory and unacceptable. The present work takes all these problems into account and provides a simple solution through the novel idea of photobioreactor design with a visible-light active heterogeneous particulate photocatalyst.

In the field of particulate photocatalyst, until recently, we have been focusing on nanostructured $CdIn_2S_4$[14] and CdS quantum dots[15] for their application to solar hydrogen production under visible light. Herein we report the new visible light photocatalyst $W_2Fe_4Ta_2O_{17}$ and its redox enzyme coupled application to a photobioreactor. Being functional under visible solar light, this device may serve as a prototype for solar fine chemical synthesis.

A schematic of the photobioreactor based on the synchronized working mechanism of photocatalysis and biocatalysis cycles is shown in Scheme 1. The photocatalyst $W_2Fe_4Ta_2O_{17}$ upon band-gap excitation by visible light ($\lambda \geq 420$ nm) promotes an electron to the conduction band (e^-_{CB}). M (an organometallic Rh complex)[11] easily receives e^-_{CB} and gets reduced. Subsequent to proton abstraction from aqueous solution, M transfers electrons and hydride to NAD^+,[11] and forms NADH (photocatalysis cycle). M, thus, shuttles as an electron mediator between photocatalyst and

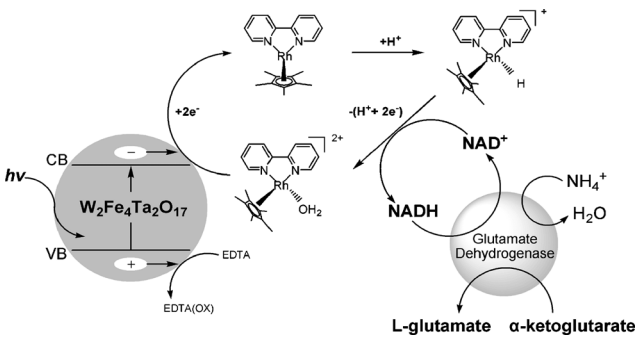

Scheme 1 Schematic diagram of the photocatalyst–enzyme coupled bioreactor functioning under visible light.

[a] *Department of Materials Science and Engineering, Korea Advanced Institute of Science and Technology, 373-1 Guseong-dong, Yuseong-gu, Daejeon, 305-701, Korea*
[b] *Department of Chemistry, Manonmaniam Sundaranar University, Tirunelveli 627 012 Tamil Nadu, India*
[c] *Center for Materials for Electronics Technology (C-MET), Panchawati, Off Pashan Road, Pune, 411 008, India*
[d] *Advanced Chemical Technology Division, Korea Research Institute of Chemical Technology, 100 Jang-dong, Yuseong-gu, Daejeon, 305-600, Korea. E-mail: jobaeg@krict.re.kr*

† Electronic supplementary information (ESI) available: Experimental details, ICP-AES chemical composition data and NADH photoregeneration time profile. See DOI: 10.1039/b808256a

NAD^+.[16] The rhodium-based organometallic compound is a promising agent for selective and efficient regeneration of NADH cofactor.[16] In the final step, NADH is consumed by α-ketoglutarate substrate for its enzymatic (glutamate dehydrogenase) conversion to L-glutamate in the biocatalysis cycle. The released NAD^+ from the enzyme can undergo photocatalysis cycle in the same way leading to the photoregeneration of NADH. The two catalysis cycles, thus, couple integrally to work together, yielding ultimately the amino acid. The hole produced in the valance band (h^+_{VB}) of the photocatalyst is nullified by an electron from a sacrificial agent such as EDTA. The activity of the photocatalyst is, thus, maintained, which, in turn, ensures the sustainable photogeneration of NADH and hence the biocatalytic synthesis of amino acid.

Photocatalyst $W_2Fe_4Ta_2O_{17}$ used in the photobioreactor was prepared by a solid-state synthesis route (see Experimental, ESI†). The XRD profile of the catalyst (Fig. 1) exhibits sharp and well defined signals that are found to be alike to a large extent to the already known profile of crystalline orthorhombic ferric tungstate (Fe_2WO_6) (JCPDS PDF # 42-0492). Accordingly, the signals are indexed to the corresponding (*hkl*) lattice planes. However, a few signals (marked by asterisks) match with the tetragonal tantalum tungsten oxide, $Ta_{16}W_{18}O_{94}$ (PDF # 29-1323). The low intensity and number of such signals suggests, however, the presence of only a negligible amount of this tetragonal phase. This observation is quite expected because of the nature of quaternary metal oxide with cations of varying ionic radii and oxidation states from 3d and 5d transition series. A similar observation for $ZnBiVO_4$ quaternary oxide with tetragonal and monoclinic systems is worth mentioning here.[17] Besides these, the profile does not show any signal from precursor oxides, indicating the formation of a single phase compound. Additionally, the single sharp peak with high intensity shows the phase purity of the compound with a high degree of crystallinity.

Morphological characterization of the photocatalyst by a field emission scanning electron microscope (FESEM) (Fig. 2) shows the presence of smooth surfaced crystalline grains of nearly oval shape with an approximate size of ≤ 1 μm. The diffuse reflectance spectrum (DRS) (Fig. 3) in the Kubelka–Munk absorbance mode demonstrates an intense light absorption up to about 600 nm with an absorption onset at 700 nm (E_g = 1.77 eV), which enables the photocatalyst to absorb maximum visible light and perform photocatalytic function.

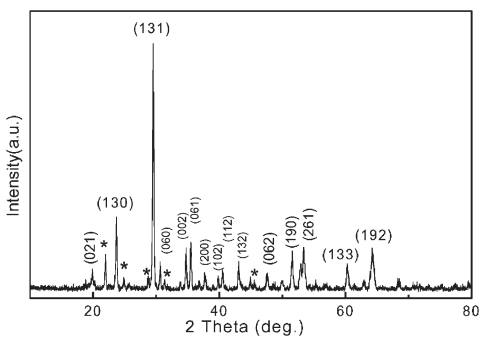

Fig. 1 XRD profile of the photocatalyst $W_2Fe_4Ta_2O_{17}$.

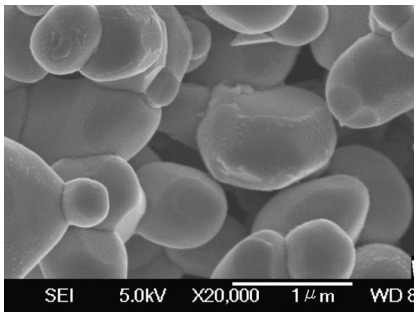

Fig. 2 FESEM image of the photocatalyst $W_2Fe_4Ta_2O_{17}$.

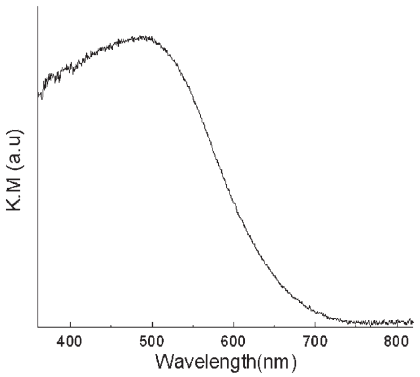

Fig. 3 DRS curve of the photocatalyst $W_2Fe_4Ta_2O_{17}$.

Elemental analysis by ICP-AES (inductively coupled plasma-atomic emission spectrometer) gives the stoichiometry of 2.0, 3.92 and 1.99 for W, Fe and Ta, respectively (see Table S1, ESI†). Being close to the initially fixed values of 2.0, 4.0 and 2.0 for the same elements, this observed stoichiometry confirms the chemical composition of the synthesized photocatalyst.

As a means of validating the proposed mechanism in Scheme 1, the functionality of photocatalysis cycle alone or the entire photobiocatalysis cycle was investigated, respectively through the evaluation of NADH photogenerated or through the evaluation of final product L-glutamate formed (see Experimental, ESI†). Also it was of interest to assess the efficiency of the present photocatalyst $W_2Fe_4Ta_2O_{17}$ against the benchmark photocatalyst TiO_2.

In NADH photogeneration, catalytic activity of our photocatalyst was tested in phosphate buffer of pH = 7.0 at room temperature (~20 °C) (details in ESI†) with different sacrificial electron donors, H_2O and EDTA (5 and 20 mM) (Fig. 4(a)). Continuous rise in NADH concentration over 14 h both with H_2O and EDTA to the levels of 0.015 mM in H_2O, 0.04 and 0.054 mM in 5.0 and 20 mM EDTA, respectively, proves the functionality of our photocatalyst. EDTA is a well-known and more powerful reducing agent than water and hence readily scavenges holes, leaving e^-_{CB} free for NAD^+ reduction. Thereby, it also prevents e^-_{CB}–h^+_{VB} recombination which is a major primary event in reducing photocatalysis efficiency. A remarkable observation is, thus, the greater hole scavenging activity of EDTA than water, resulting in roughly a two- to three-fold increase in NADH yield compared to that in water. Nevertheless, this observation pinpoints the fact that our photocatalyst $W_2Fe_4Ta_2O_{17}$ performs its role in aqueous medium also even

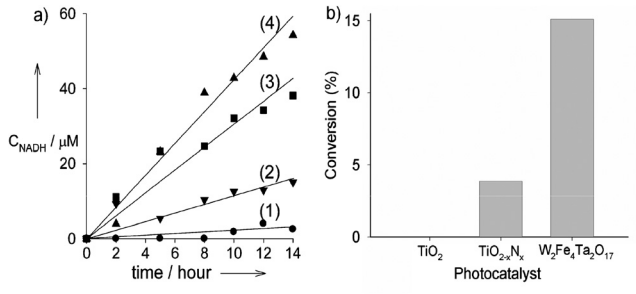

Fig. 4 (a) NADH photoregeneration time profiles over 14 h period of (1) TiO_2 with 5 mM EDTA, (2) $W_2Fe_4Ta_2O_{17}$ with H_2O, (3) and (4) $W_2Fe_4Ta_2O_{17}$ with 5 and 20 mM EDTA, respectively; (b) L-Glutamate synthesis over 24 h period with 5 mM EDTA in the presence of $W_2Fe_4Ta_2O_{17}$, $TiO_{2-x}N_x$ and TiO_2, respectively.

without any deliberately added electron donor. On the other hand, the benchmark photocatalyst TiO_2, even with EDTA, could show only a lesser efficiency, because of its poor visible light absorption and photosensitization process.

NADH photogeneration when studied for 24 h (Fig. S1 and S2, ESI†), shows there is almost time-linearity for our photocatalyst with an accumulated NADH production of 0.065 mM, amounting to 65% conversion of NAD. TiO_2, however, produced only a meagre amount (<0.004 mM) with a profile almost parallel to the time axis. Collectively, all these NADH time profiles (1) confirm the operation of photocatalysis cycle, (2) reveal the photostability and durability of our catalyst and (3) highlight its greater efficiency than the benchmark TiO_2.

Fig. 4(b) shows the graph of percentage conversion of α-ketoglutarate to L-glutamate. Our catalyst $W_2Fe_4Ta_2O_{17}$ achieved about 15% conversion of α-ketoglutarate with EDTA (5 mM) hole scavenger while the other visible light photocatalyst $TiO_{2-x}N_x$ ($x = 0.01$)[18] gave only 4%, and TiO_2 exhibited absolutely no yield. Components such as glutamate dehydrogenase, cofactor, and redox-mediator were stable under reaction conditions, which was attributed to the sacrificial protection by the reductant (EDTA) against the hole oxidation. Moreover, the photobiosynthesis of glutamate with our catalyst showed non-equilibrium behavior until 10 h duration. The bioreactor, thus, functions heterogeneously. Since photocatalysis and biocatalysis cycles work synchronously, the co-factor is consumed as soon as it is formed and the product is synthesized continuously. The after-generation utility of NADH is, thus, accomplished in the photobioreactor design. Consequently, the thermodynamic equilibrium of NADH photogeneration is shifted towards the product side, which is a remarkable feature of the present system. Moreover, since the system is heterogeneous, the photocatalyst and the product are easily separable. Thus it is possible to maintain the thermodynamic equilibrium always to the product side and hence to sustain the photobiosynthesis. The photobioreactor design, thus, removes major problems of the previous photocatalytic systems. Chiefly, with appropriate enzyme and substrate, the present photobioreactor also makes the synthesis of tailor made fine chemicals feasible. Thus, the present work demonstrates successfully a new and potentially promising visible-light driven artificial photosynthesis system for the ultimate goal of utilization of solar energy in fine chemical synthesis.

This work was supported by Korea Science and Engineering Foundation (KOSEF) NRL Program grant from the Korea Government (MEST) (No. R0A-2008-000-20041-0).

Notes and references

1 (*a*) T. J. Meyer, *Nature*, 2008, **451**, 778–779; (*b*) R. Konduri, H. Ye, F. M. MacDonnell, S. Serroni, S. Campagna and K. Rajeshwar, *Angew. Chem., Int. Ed.*, 2002, **41**, 3185–3187; (*c*) G. Palmisano, V. Augugliaro, M. Pagliaro and L. Palmisano, *Chem. Commun.*, 2007, 3425–3437.
2 K. Sayama, K. Mukasa, R. Abe, Y. Abe and H. Arakawa, *J. Photochem. Photobiol., A*, 2002, **148**, 71–77.
3 L. Hammarstroem, *Curr. Opin. Chem. Biol.*, 2003, **7**, 666–673.
4 O. Diwald, T. L. Thompson, T. Zubkov, G. Goralski, S. D. Walck and J. T. Yates, Jr, *J. Phys. Chem. B*, 2004, **108**, 6006–6008.
5 K. M. Koeller and C.-H. Wong, *Nature*, 2001, **409**, 232–240.
6 Z. Jiang, C. Lu and H. Wu, *Ind. Eng. Chem. Res.*, 2005, **44**, 4165–4170.
7 S. K. Yoon, E. R. Choban, C. Kane, T. Tzedakis and P. J. A. Kenis, *J. Am. Chem. Soc.*, 2005, **127**, 10466–10467.
8 Z. Goren, N. Lapidot and I. Willner, *J. Mol. Catal.*, 1988, **47**, 21–32.
9 W. A. Donk and H. Zhao, *Curr. Opin. Biotechnol.*, 2003, **14**, 421–428.
10 J. Wang, P. V. A. Pamidi and M. Jiang, *Anal. Chim. Acta*, 1998, **360**, 171–178.
11 H.-K. Song, S. H. Lee, K. Won, J. H. Park, J. K. Kim, H. Lee, S. J. Moon, D. K. Kim and C. B. Park, *Angew. Chem., Int. Ed.*, 2008, **47**, 1749–1752.
12 Y. Amao and T. Watanabe, *J. Mol. Catal. B: Enzym.*, 2007, **44**, 27–31.
13 T. Sagawa, R. Sueyoshi, M. Kawaguchi, M. Kudo, H. Ihara and K. Ohkubo, *Chem. Commun.*, 2004, 814–815.
14 B. B. Kale, J.-O. Baeg, S. M. Lee, H. Chang, S.-J. Moon and C. W. Lee, *Adv. Funct. Mater.*, 2006, **16**, 1349–1354.
15 B. B. Kale, J.-O. Baeg, S. K. Apte, R. S. Sonawane, S. D. Naik and K. R. Patil, *J. Mater. Chem.*, 2007, **17**, 4297–4303.
16 F. Hollmann, A. Schmid and E. Steckham, *Angew. Chem., Int. Ed.*, 2001, **40**, 169–171.
17 B. B. Kale, J.-O. Baeg, J. S. Yoo, S. M. Lee, C. W. Lee, S. J. Moon and H. Chang, *Can. J. Chem.*, 2005, **83**, 527–532.
18 (*a*) R. Asahi, T. Morikawa, T. Ohwaki, K. Aoki and Y. Taga, *Science*, 2001, **293**, 269–271; (*b*) S. In, A. Orlov, F. Garcia, M. Tikhov, D. S. Wright and R. M. Lambert, *Chem. Commun.*, 2006, 4236–4238.